Multiscale Modeling of Surfactant Phase Behavior in the Remediation of DNAPL Contamination

Xiangyu Fan

A thesis submitted to the faculty of the University of North Carolina at Chapel Hill in partial fulfillment of the requirements for the degree of Master of Science in the Department of Environmental Science and Engineering, School of Public Health.

Chapel Hill
2008

Approved by:

Advisor: Dr. Cass T. Miller

Reader: Dr. Max L. Berkowitz

Reader: Dr. Joseph A. Pedit

ABSTRACT

Xiangyu Fan: Multiscale Modeling of Surfactant Phase Behavior in the Remediation of DNAPL contamination
(Under the direction of Cass T. Miller)

The brine barrier remediation technique (BBRT) has been proposed as a novel Brine barrier remediation techniques (BBRT) that use surfactants have been proposed for remediating subsurface environments contaminated by dense non-aqueous phase liquids (DNAPLs). Their successful implementation requires an understanding of surfactant phase behavior including surfactant accumulation at the water/DNAPL interface and surfactant precipitation due to the presence of high aqueous-phase concentrations of brine. Multiscale modeling based upon thermodynamics and molecular dynamics (MD) was performed to investigate surfactant precipitation and molecular details at the surfactant-modified water/DNAPL interface. While these modeling results advance the understanding of surfactant behavior, a few open issues must be addressed before these new methods can be considered reliable and mature.

ACKNOWLEDGEMENTS

First of all, I would like to thank my advisor, Professor Cass T. Miller for his careful guidance and continuous support to my research in the past two years. I have learned from him not only knowledge in science, but also the way to be a successful person. It is hard to imagine that I can finish my master study without the warm-hearted help from him.

I would also like to thank my committee member Professor Max L. Berkowitz and Dr. Joseph A. Pedit in my master committee for their time and encouragement.

I would also like to thank Dr. Lanyuan Lu and Zhancheng Zhang in the Chemistry department, Dr. Shubing Wang and CD Poon at ITS for their advice on my MD simulation work.

There are many people who have helped me with my research work in my department. I thank some graduate students: Stephen Richardson and Hongbo Zhu in Professor Aitken's group, and Patrick M. Sanderson, Pamela Birak, Aren Newman and Benjamin Lebron in my group. I especially thank Emmie Granbery for her encouragement during my graduate study.

Finally, I would thank my parents in China, for their continuous support during my two years of graduate study.

TABLE OF CONTENTS

LIST OF FIGURES

LIST OF ABBREVIATIONS AND SYMBOLS

BBRT	Brine barrier remediation technique
^0C	Degrees Celcius
$CaCl_2$	Calcium chloride
CMC	Critical micelle concentration
cmc_{MA}	Critical micelle concentration of MA-80
cmc_{Tr}	Critical micelle concentration of Triton X-100
DNAPL	Dense nonaqueous phase liquid
g	gram
GAFF	General amber force field
GROMACS	GROningen MAchine for Chemical Simulations
I	Ionic strength of surfactant solution (M)
IFT	Interfacial tension
K_1	Constants in MA-80 CMC Modification
K_g	Constants in MA-80 CMC Modification
K_{sp}	Solubility product constant of MA-80 in Ca salt solution
L	Liters
m	Meter
M	Molarity (moles/Liter)
MA-80	Sodium dihexyl sulfosuccinate
MD	Molecular dynamics
mL	Milliliter
nm	Nanometers
PCE	Tetrachloroethylene
Triton X-100	Polyoxyethylene octylphenol

x_{MA}	Fraction of MA-80 on mixed micelles
ρ	Density (kg/L)
γ_{Ca}	Activity coefficient of Ca ions in solution
γ_{MA}	Activity coefficient of MA-80 ions in solution
β_{Ca}	Binding ratio of Ca ions on micelles
β_{Na}	Binding ratio of Na ions on micelles
β	Interaction coefficient in micelles (Non-ideal mixture)

1 INTRODUCTION

The remediation of subsurface systems contaminated with DNAPL contaminants is frequently inefficient and expensive when employing conventional technologies like pump-and-treat (PAT) due to very low solubilities and dissolution rates of DNAPLs in water (1-3). Various surfactant-enhanced aquifer remediation (SEAR) techniques have been developed to combat these problems and SEAR techniques have been demonstrated to be capable of enhancing the remediation performance through lowering interfacial tension, solubilizing DNAPLs into micelles, and accelerating mass transfer to the mobile aqueous phase (4-10). However, SEAR techniques that significantly lower water/DNAPL interfacial tension increase the possibility of mobilizing DNAPL into fine-textured or uncontaminated aquifer material (11,12). Brine barrier remediation technologies (BBRT) have been proposed for minimizing the negative impacts of uncontrolled surfactant-induced DNAPL mobilization. BBRTs involve injection of brine with a density greater than that of DNAPL into the bottom of a remediation zone. One variant of BBRTs would then use a surfactant flush above the established brine barrier to promote downward DNAPL mobilization. The mobilized DNAPL would become trapped in the upper reaches of the brine barrier where it would be recovered once DNAPL saturation became large enough to allow the DNAPL to be pumped to recovery wells (12-14).

In our previous studies (12-14), several related remediation technologies based upon the coupling of brines and surfactants were carefully investigated in bench-scale experiments. We examined DNAPL solubilization, migration, and recovery in one-, two-, and three-dimensional systems (12,13) and were able to achieve near-complete

DNAPL removal from heterogeneous sands using BBRTs followed by vapor extraction (14). The surfactant solution used in those studies contained a mixture of sodium diamyl sulfocuccinate (Cytec Industries, Aerosol® AY) and sodium dioctyl sulfosuccinate (Cytec Industries, Aerosol® OT). Unfortunately, the anionic surfactants in the solution were prone to precipitation when mixed with calcium-based brine solutions like calcium bromide. Precipitated surfactant can clog pores in unconsolidated subsurface media and well screens. More recent laboratory and field studies (unpublished) modified the surfactant solution to make it less prone to precipitation problems by addition of a nonionic surfactant. The modified solution contained sodium dihexyl sulfosuccinate (Cytec Industries, Aerosol® MA 80-I, an anionic surfactant), octylphenol ethoxylate (Dow Chemical, Triton™ X-100, a nonionic surfactant), isopropanol, and calcium chloride. The modified solution worked as desired in the laboratory and field studies, but a labor-intensive series of phase-behavior experiments was required to find the appropriate mixture.

The use of models based upon thermodynamics and molecular dynamics may help reduce the amount of laboratory effort needed to find surfactant solutions appropriate for environmental remediation. Thermodynamic modeling has been successfully used to explain surfactant precipitation in the presence of cationic and nonionic species (15, 16-22). Despite this success, the related work has not addressed surfactant mixtures used in subsurface remediation. Moreover, the models for mixed surfactant systems mainly originated from the Poisson-Boltzmann equation (17,23,24), which is difficult to solve due to the involvement of micellar surface properties (17) in the model. In recent years, MD modeling has been used to understand the underlying physics of various surfactant-modified interfaces (25-30). Unfortunately, as with thermodynamic modeling approaches, the related work has rarely addressed the field

of environmental remediation. Currently, surfactant selection for environmental remediation relies on a large amount of repeated experiments (31). Even when experiments yield appropriate surfactants for an application, the experiments often fail to explain positive results due to the lack of information at the molecular level. Considering the variability and complexity of remediation systems, it is important to develop simplified thermodynamic models and molecularly informative MD models to aid in research related to BBRTs and SEAR.

The goal of this work is to study surfactant phase behavior as it relates to the remediation of DNAPL-contaminated subsurface systems using BBRTs. The specific objectives of this work are (i) to use simplified thermodynamic models to describe the conditions under which precipitation occurs when the surfactant mixture (i.e., Aerosol® MA 80-I and Triton™ X-100) is in the presence of a salt-derived divalent cation (i.e., calcium from calcium chloride or calcium bromide); (ii) to use MD models to visualize microscale structure, calculate interfacial tension at the water/DNAPL interface when different types of surfactants are present, and compare their performance; and (iii) to assess the potential of computer-assisted surfactant selection and the feasibility of studying surfactant precipitation using MD models.

2 METHODS

2.1 Model Formulation

As discussed earlier, our recent experiments have used a surfactant mixture containing Aerosol® MA 80-I and Triton™ X-100 (hereafter the anion of Aerosol® MA 80-I formed on dissolution will be referred to as MA, and Triton™ X-100 will be referred to as simply Triton) to promote DNAPL mobilization through a reduction of tension at the water/DNAPL interface. Calcium chloride ($CaCl_2$) was added to the mixture to help control Winsor type formation for producing the highest mobility potential always accompanied by Winsor Type III (32). Isopropanol was added to facilitate breaking of macroemulsions and to decrease microemulsion viscosity (33). Tetrachloroethylene (PCE) was selected as a representative DNAPL. Aqueous solutions of calcium bromide ($CaBr_2$) can achieve densities exceeding PCE's density of 1.63 g/mL, so it was chosen as being an electrolyte suitable for use as a brine barrier for arresting the vertical migration of PCE.

The model development that follows is expressed in terms of the concentrations of the chemical species discussed above instead of more general terms for the sake of simplicity. For such a system, MA monomers may precipitate with free calcium ions that come from the calcium bromide present in the brine barrier and the calcium chloride present in the surfactant mixture. MA and Triton monomers will aggregate to produce mixed micelles once the critical monomer concentration (CMC) is exceeded. Part of the free calcium and sodium ions will associate with the micelles due to electrostatic attraction and be considered bound for modeling purposes.

Solubility product theory has been used to describe surfactant precipitation

(17-18) and for the system under consideration can be expressed as

$$K_{sp} = \left[Ca^{2+}\right]_u \left[MA^-\right]_{mo}^2 \gamma_{Ca}\gamma_{MA}^2 \quad \textbf{(1)}$$

where $[Ca^{2+}]_u$ is the concentration of unbound calcium ions; $[MA^-]_{mo}$ is the concentration of MA monomers; γ_{Ca} and γ_{MA} are the activity coefficients for unbound calcium ions and MA monomers, respectively. Depending upon the ionic strength of the solution, the activity coefficients can be approximated by the Extended Debye-Hückel or Davies equations (34). From previous study, much higher concentration of Na^+ is needed to cause ionic surfactant precipitation when compared with Ca^{2+} (17). Therefore, MA precipitation with Na^+ is ignored in this work, considering low concentration of Na^+ present in system.

In order to quantify the binding of counter ions to the micelles, binding ratios (35) for calcium and sodium ions are defined as

$$\beta_{Ca} = 2\left[Ca^{2+}\right]_b / \left[MA^-\right]_{mi} \quad \textbf{(2)}$$

$$\beta_{Na} = \left[Na^+\right]_b / \left[MA^-\right]_{mi} \quad \textbf{(3)}$$

where $[MA^-]_{mi}$ is the concentrations of MA present in the micelles, respectively; and $[Ca^{2+}]_b$ and $[Na^+]_b$ are the aqueous concentrations of calcium and sodium ions associated with the micelles, respectively.

The non-ideal mixing formula was selected for bridging the aqueous and micelle phases due to its wide use in describing binary mixed surfactant systems (36), which when coupled with the assumption of a regular solution (15) gives

$$\left[MA^-\right]_{mo} = cmc_{MA} \exp\left[\beta\left(1-x_{MA}\right)^2\right] x_{MA} \quad \textbf{(4)}$$

$$\left[Tr\right]_{mo} = cmc_{Tr} \exp\left(\beta x_{MA}^2\right)\left(1-x_{MA}\right) \quad \textbf{(5)}$$

where $[Tr]_{mo}$ is the aqueous concentration of Triton monomers; cmc_{MA} and cmc_{Tr} are

the CMC of MA and Triton, respectively; x_{MA} is the mole fraction of MA in the mixed micelles; and β is a dimensionless interaction parameter used to describe non-ideality in the mixed micelles.

The effect of unbound sodium and calcium ions on the CMC of MA needs to be included in the model formulation, adequately quantified (37) by

$$\ln cmc_{MA} = K_1 - K_g \ln\left[X\right]_u \quad \textbf{(6)}$$

where K_1 and K_g are constants; $[X]_u$ is the aqueous concentration of an unbound counterion which has same effect on MA CMC as does the mixture of unbound sodium and calcium ions.

The variable of interest in the model is the minimum concentration of total calcium ions required to cause surfactant precipitation (*i.e.*, the precipitation boundary). When the total concentrations of MA and Triton are given, the system of equations outlined above, along with mass conservation equations for the surfactants, can be easily solved if $[X]_u$ in Equation 6 is resolved. If an unbound calcium ion is assumed to have the same effect on the CMC of MA as two unbound sodium ions, then

$$\left[X\right]_u = \left[Na^+\right]_u + 2\left[Ca^{2+}\right]_u \quad \textbf{(7)}$$

The simplification is plausible because Ca^{2+} has a similar charge density by weight with Na^+. Based upon the above description, it should be possible to calculate the precipitation boundary for any combined surfactant concentration and MA/Triton ratio if the model parameters (*i.e.*, cmc_{Tr}, β, K_1, K_g, β_{Ca}, β_{Na}, and K_{sp}) are known. These parameters were determined sequentially as is described below.

2.2 Experimental Methods

2.2.1 Materials

Aerosol® MA 80-I and Triton™ X-100 were used as received from Cytec

Industries (West Paterson, NJ) and Acros Organics (Geel, Belgium), respectively. They were 80 and 100% effective, respectively. All concentrations refer to the effective amount of MA or Triton. The sodium chloride, calcium chloride, and calcium bromide used were reagent grade (Fisher Scientific, Pittsburgh, PA) and the water used was distilled and deionized.

2.2.2 CMC Determination

CMC was inferred from surface tension measurements. For a given set of experiments, the surface tension was measured as a function of total surfactant concentration. The CMC was estimated from the intersection of the descending and plateau parts in the curve obtained by plotting surface tension as a function of total surfactant concentration (38). A DuMoüy interfacial tensiometer (Central Scientific, Fairfax, VA) was used to measure surface tension. All of the measurements were repeated until a stable reading was obtained.

To study the interaction between MA and Triton, eight groups of experiments were performed to determine CMC as a function of the molar ratio of the surfactants. Similarly, for examining the effects of dissolved salt, six groups of experiments were conducted to determine the CMC of MA as a function of the amount of sodium chloride in solution. The collection of estimated CMC values in conjunction with Equations 4, 5, and 7 can be used to separately estimate parameter values for parameters β, K_1, and K_g.

2.2.3 Precipitation Boundary Determination

A visual method (17) was used to determine the precipitation boundary. A series of solutions with identical surfactant concentrations, but with varying calcium chloride concentrations, were prepared in 100-mL volumetric flasks. All solutions were cooled to 4º C to promote precipitation. The solutions were then placed in a 25º C

constant temperature room, shaken periodically, and allowed to equilibrate for four days. If precipitate was observed after equilibration, the solution was deemed to be within the precipitation boundary. The gradations in the varied calcium chloride concentrations were fine enough such that the precipitation boundary could be determined to within 5 % for the single surfactant solutions and to within 10% for the mixed surfactant systems.

2.3 MD Simulations

Several molecular dynamics simulations were performed to understand phase behavior at the water/DNAPL interface. A MD simulation of a simple system containing only water and PCE was performed to test if the modeling could accurately predict the interfacial tension between water and PCE. The bulk of the simulations involved systems containing water, PCE, and a surfactant to examine reductions in interfacial tension and help visualize the micro structure at the water/PCE interface when modified by the presence of a surfactant. MA or Triton molecules and examine IFT decrease in these cases. Additional simulations were performed for systems containing MA and Triton to examine their interactions at the water/PCE interface.

The simulated system had a cross section 2.9 nm × 2.9 nm in the x-y plane and contained 250 PCE molecules, 1458 water molecules, and a variable number of surfactant molecules. Average molecular distance in the simulated system was set such that he overall density in the simulated system was approximately the same an identical real system. Periodic boundary conditions were used which led to the formation of two water/PCE interfaces in the simulated system. To minimize spatial error, the surfactant molecules' initial positions were evenly distributed on the lattices of the two interfaces with their head/tail group (*i.e.*, ionized/unionized group in MA and polyethylene oxide/hydrocarbon group in Triton) toward the water/ PCE,

respectively.

The Simple Point Charge - Extended (SPC/E) model was used to describe the water molecule due to its accuracy at normal room temperature (39). General AMBER force field (GAFF) parameters were used to describe the surfactant and PCE molecules because GAFF covers the most common atoms and has demonstrated reliability (40). The HF/6-31G* RESP charge method (41) was used to calculate atomic point charges.

MD simulations were accomplished using the GROMACS (Groningen Machine for Chemical Simulations) package. The simulations were performed under a constant normal pressure of 1 bar along the z axis and a constant temperature of 300 K**.** The initial velocities of the atoms were set according to a Maxwellian distribution (42). The initial pressure and temperature were held constant through the simulation through coupling to the Parrinello-Rahman barostat (43) and the Berendsen thermostat (44) with a relaxation time of 0.5 picoseconds. The length of each simulation was 30 nanoseconds, 20 nanoseconds for equilibration and 10 nanoseconds for data collection. The water/PCE interfacial tension for each simulation was calculated using the pressure difference formula (27) after taking into account the formation of two interfaces in the simulated systems.

3 RESULTS AND DISCUSSION

3.1 Surfactant Precipitation Boundary

In this section, thermodynamic modeling was used to describe MA precipitation due to the presence of salts. The parameters β, K_1, K_g, β_{Ca}, β_{Na} and K_{sp} were determined sequentially. The resulting model was verified through comparisons with experimental data.

3.1.1 Estimation of Parameters

The CMC of surfactant mixture, expressed as the summation of MA and Triton monomer concentrations, can be identified where surface tension (ST) breaks. Using the strategies previously mentioned, the CMC under a given mixture condition was determined and presented in Figure 3.1.

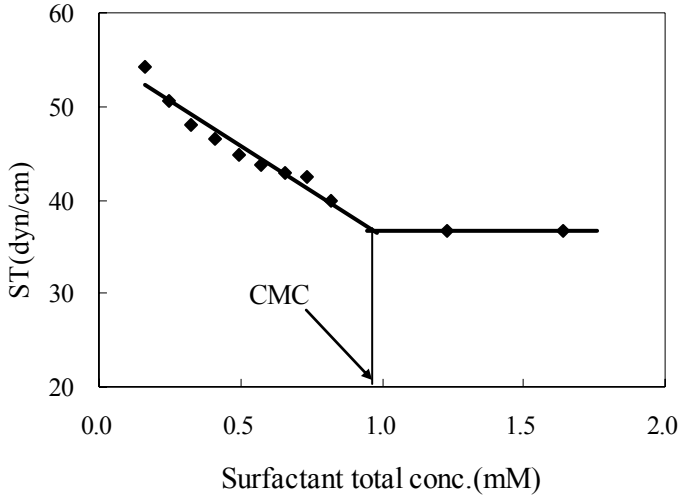

Figure 3.1 CMC determination of mixed surfactants (MA:Triton=7.2:1)

Figure 3.2 shows the CMC as a function of MA mole fraction of the surfactant mixture without the addition of salts. The surfactant monomer concentrations were determined from Equations 4 and 5. A fit of the data to the model yielded an optimal β

estimate of -3.7 where the global error between them was minimized.

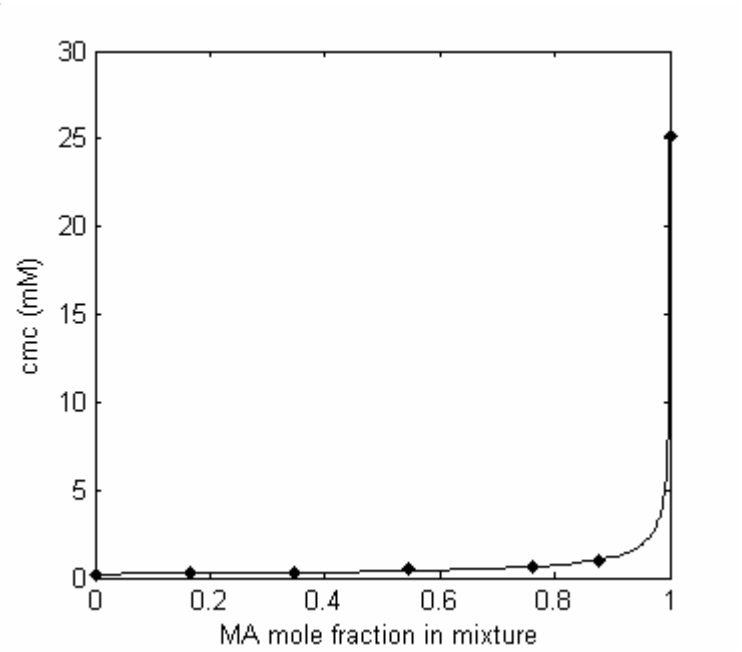

Figure 3.2 Comparison of data and model fit of CMC as a function of MA mole fraction

The CMC of MA as a function of the aqueous-phase concentration of sodium ion is shown in Figure 3.3. The sodium ions were derived from the dissolution of the surfactant and the addition of sodium chloride. The best fit of Equation 6 to the data yields parameter estimates of -4.3475 and 0.1806 for K_1 and K_g, respectively.

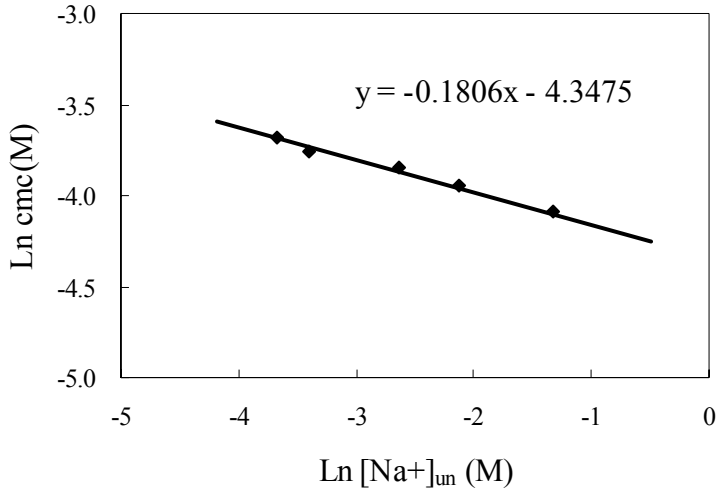

Figure 3.3 Comparison of data and model fit for the CMC of MA as a function of sodium ion concentration

The potential measured by a sodium ion selective electrode is indicative of the free

sodium ion concentration in solution (36). Using an electrode method, the binding fraction of sodium ions, β_{Na}, was determined to be 0.32 for MA surfactant solutions. Calcium ions compete with sodium ions in associating with MA micelles when introduced in the mixture (36). It is assumed that the same fraction of MA micelle charges is neutralized for mixed counterion solutions as for single counterion solutions (17). Based upon this assumption, β_{Ca} and β_{Na} were calculated to be 0.29 and 0.32, respectively, in solutions containing sodium and calcium ions.

MA solutions with concentrations below the CMC (0.025 M) were used to determine the solubility product. Figure 3.4 shows the experimental data and the model (i.e., Equation 1) fit to the data. Depending on ionic strength, Davies equation was used to estimate activity coefficients for the MA and calcium ions. The value of the solubility product was $2.9\times10^{-6}M^3$. In contrast, the solubility product of MA^- and Na^+ is roughly estimated as $0.78M^2$ directly from MA solubility of 343 g/L (25º C). It indicates the solubility product based on Na^+ should still be much larger than that based on Ca^{2+} after adding the effects of activity. This result partially verified the assumption that MA^- precipitation with Na^+ can be ignored in such a system.

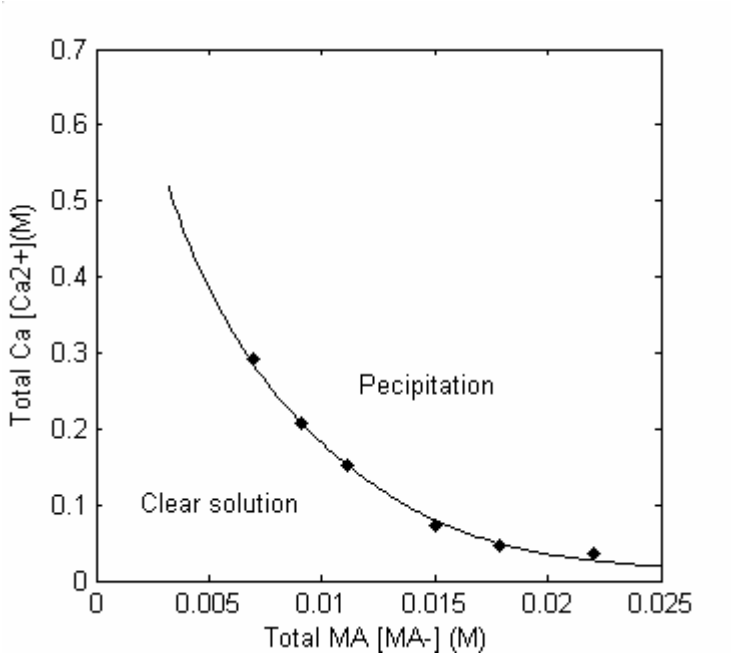

Figure 3.4 Precipitation boundary of MA below CMC (K_{sp}=2.9×$10^{-6}M^3$)

3.1.2 Model Verification

MA systems with and without Triton and above the CMC were modeled using the estimated model parameters to test the validity of the modeling approach.

(1) MA system above the CMC without Triton

The results shown in Figure 4 demonstrate a solubility product of $2.9\times10^{-6}M^3$ adequately describes the MA precipitation boundary below the CMC for solutions without Triton present. As shown in Figure 3.5, the model also accurately predicts the precipitation boundary that was experimentally observed over CMC. The relative error between the model and data was less than 5 percent, except near the CMC.

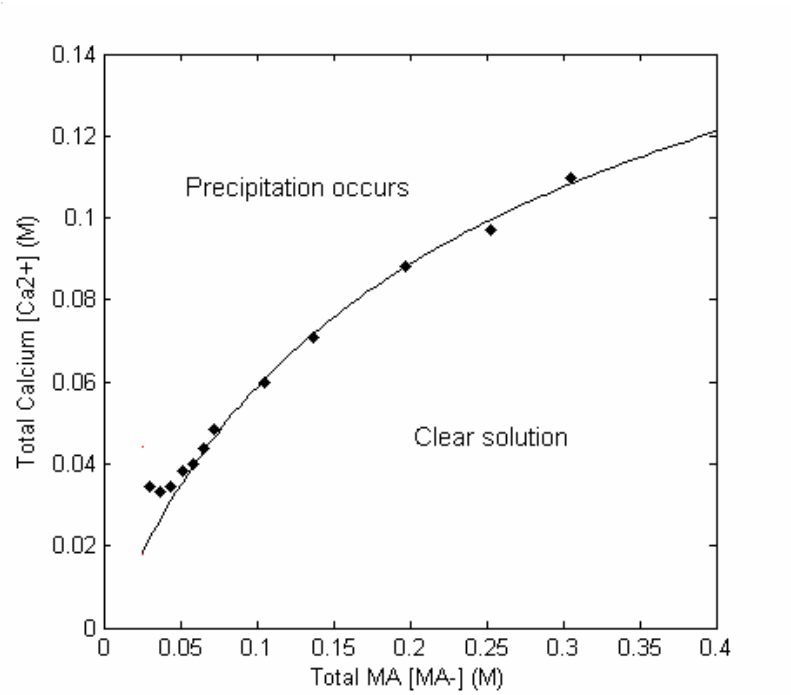

Figure 3.5 MA Precipitation boundary above the CMC without Triton

As noted above, the predicted precipitation boundary deviates from the experimental data near the CMC. CMC determination for MA is not without issues. Figure 3.6 shows surface tension as a function of MA concentration for a system without additional salts or Triton present. The descending portion of the data is never well-represented as a straight line, even at the lowest MA concentrations. As a result, CMC estimated by the intersection of straight lines through the descending and plateau sections of the data is not much better than a guess. Also, the amount of alcohol in the system is directly related to the MA concentration because the Aerosol® MA 80-I used in this study contains approximately 5% isopropanol. The presence of alcohol further complicates the behavior of the system. Results similar to those seen for MA in this work have been reported elsewhere (17).

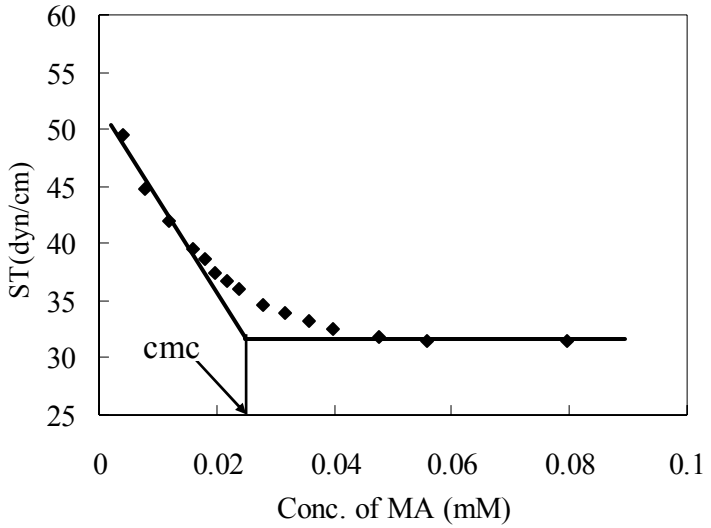

Figure 3.6 Surface tension as a function of MA concentration

(2) MA system with Triton

Multiple substitutions involving Equations 1 through 7 were required to generate a system of equations reliant on two master variables for predicting the precipitation boundary for a system containing MA and Triton. The master variables are the mole fraction of MA in the micelles and the total calcium ion concentration in solution. The relevant equations are

$$-\log K_{sp} + \log\left[Ca^{2+}\right]_u + 2\log\left[MA^-\right]_{mo} + 2\log\gamma_{MA} + \log\gamma_{Ca} = 0 \qquad \textbf{(8)}$$

$$\ln\left[MA^-\right]_{mo} - \ln x_{MA} - \beta\left(1-x_{MA}\right)^2 - K_1 + K_g \ln\left(2\left[Ca^{2+}\right]_u + \left[Na^+\right]_u\right) = 0 \qquad \textbf{(9)}$$

where $[MA^-]_{mo}$, $[Ca^{2+}]_u$, and $[Na^+]_u$ are functions of the two master variables. Figure 3.7 compares experimental data with model predictions based on Equations 8 and 9 for two systems with MA:Triton ratios of 95:5 and 90:10. The model predictions follow the general data trends up to 0.2M MA and are comparable to previously reported modeling predictions of similar mixed surfactant systems (17, 18), but require fewer parameters and calculations.

The moderate success shown above for predicting the precipitation boundary for mixed surfactant systems is a promising first step in using such modeling to aid in developing mixed surfactant solutions for use in brine barrier based technologies. A

few issues are worthy of further study to improve the reliability of the model predictions. Both counterions and nonionic surfactants may change the fraction of ion binding on ionic surfactant micelles (36, 15), so the variation of the ion binding parameter with solution conditions warrants further study. Increasing the ionic strength can decrease the magnitude of the interaction parameter in many ionic/nonionic surfactant mixtures (15), so the variation of the interaction parameter with ionic strength also warrants further study.

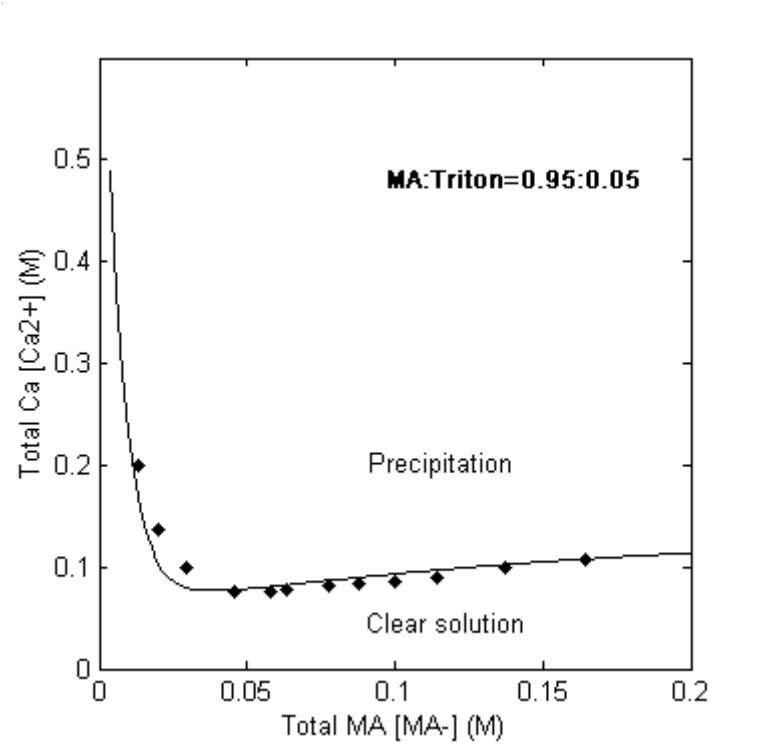

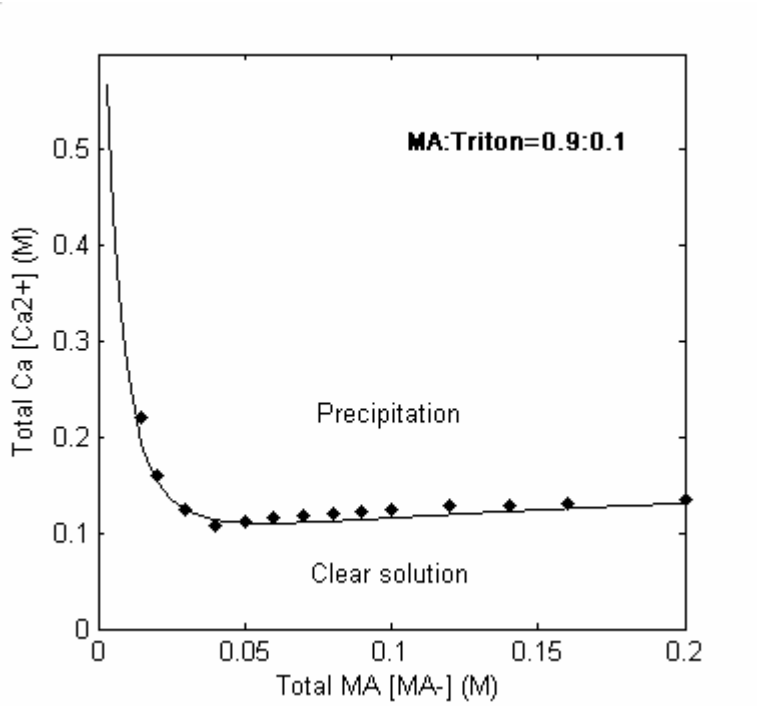

Figure 3.7 MA precipitation boundary for two MA:Triton ratios

3.2 MD Simulations of Surfactant Phase Behavior

In this section, the results of MD simulations of the phase behaivor of MA and Triton are discussed. All of the simulations are similar so only one representative system involving 8 MA molecules is discussed to detail characteristics common to all of the simulations.

Figure 3.8 shows the three-dimensional configuration of a MA ion created accroding to its basic molecular structure. MA has two parallel hydrocarbon branches in its hydrophobic tail. Figure 3.9 shows a micelle formed in the simulation of a system containing only MA and water. The MA ions that make up the micelle formed in the simulation have the correct orientation with their hydrophilic heads pointed outward into the aqueous phase and their hydrophobic tails pointed inward.

Figures 3.10a and 3.10b show the simulated system in its initial and final states, respectively. As the simulation progresses from its initial state, water and PCE molecules migrate toward one another. To visualize MA anions at the final state, the other species are removed and the result shown in Figure 3.10c. All the surfactant

anions are in the correct orientation with their hydrophilic heads pointed into the aqueous phase and their hydrophobic tails pointed into the DNAPL. The MA anion located to the far right in Figure 3.10c is associated with the interface on the left side. The separation may be attributed to the periodic boundary condition used. In a similar fashion, all of the other simulations were constructed as indicated by Figures 3.8 through 3.10.

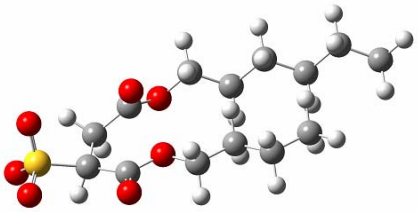

Figure 3.8 MA^- structure. Color scheme: yellow balls, sulfur atoms; red balls, oxygen atoms; grey balls, carbon atoms; white balls, hydrogen atoms.

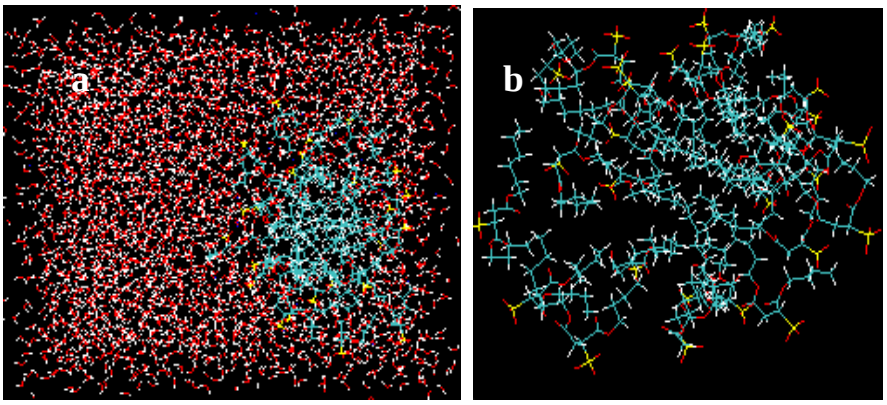

Figure 3.9 (a) System with all species shown. (b) Close up view of MA ions making up the micelle. The color scheme is the same as indicated in Figure 3.8.

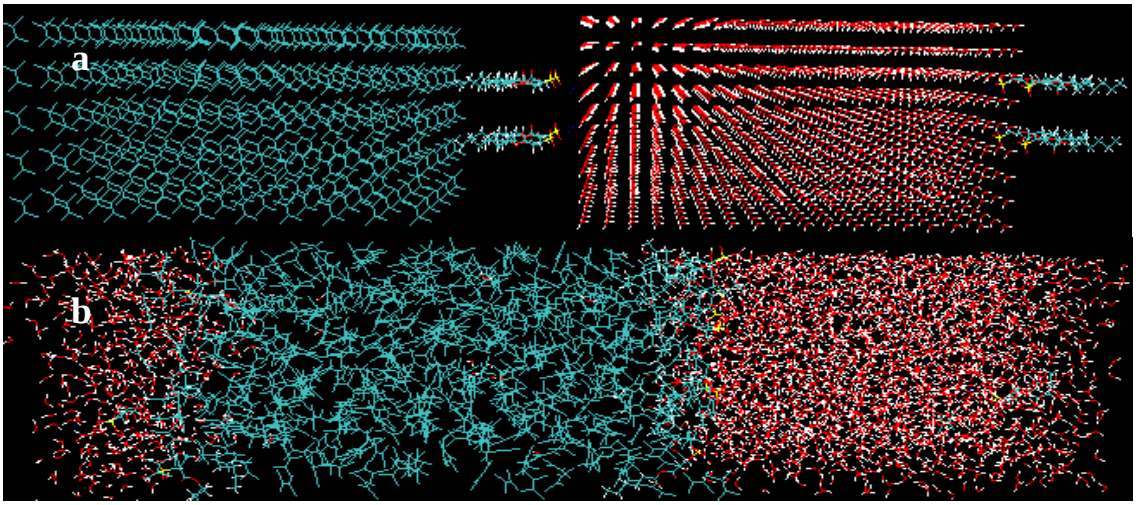

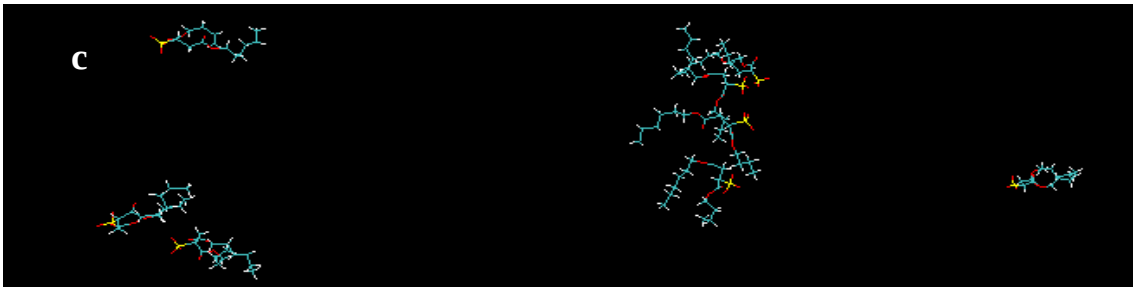

Figure 3.10 System containing water, PCE and MA. (a) Initial conditions for the simulation. (b) Final state of the simulation. (c) Final state of the simulation showing just the MA ions. MA system in different stages. Structures completely green in (a) and (b) are PCE.

The water/PCE interfacial tension was calculated from the final state for each simulation, with the results for the systems containing water, PCE, and a variable number of surfactant molecules shown in Figure 3.11. The IFT decreases with the number of surfactant molecules in the system for both Triton and MA. This trend is as expected because these surfactants were originally selected as additives to decrease IFT between the aqueous phase and DNAPL. Figure 3.12 shows the overall density of the simulated systems as a function of the number of surfactant molecules. The water/PCE mixture (ρ=1.26 kg/m^3) is denser than MA (ρ=1.13 kg/m^3) and Triton (ρ=1.07kg/m^3), so the overall density of the system would be expected to decline with surfactant addition if there were no change in volume with mixing.

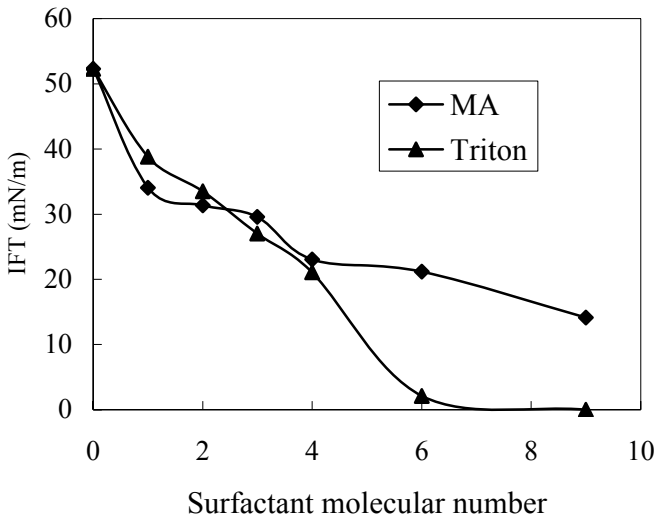

Figure 3.11 Water/PCE interfacial tension as a function of the number of surfactant molecules.

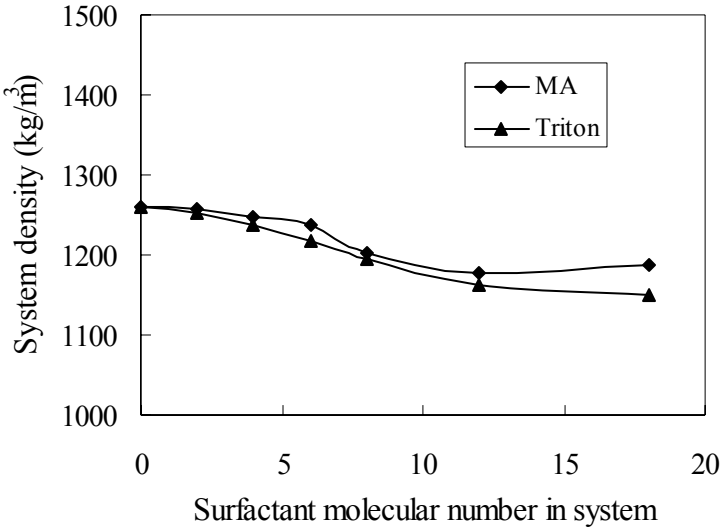

Figure 3.12 Overall density of the simulated systems as a function of the number of surfactant molecules.

There are IFT measurements in the literature for systems similar to those represented in Figure 3.11. The water/PCE IFT without surfactants present was 51.5mN/m in the MD simulation versus a measured value of 47.5mN/m for the same system (45). It has been reported (46, 47) that the interfacial tensions of 4% (w/w) surfactant solutions were 15 and 1.96 mN/m for Triton and MA, respectively. 4% (w/w) corresponds to 4.5 Triton molecules or 7.2 MA molecules in the simulated system. From Figure 3.11, the IFTs for 4% (w/w) would be approximately 15 and 20 mN/m for Triton and MA, respectively. The great difference between experimental and simulation results should be expectable because such constructed system can not be amplified to be a real system through simply multiplying its volume. There may be dynamic concentration equilibrium between bulk solution and interface. Moreover, from IFT variation trend presented in Figure 3.11, 15 MA molecules are capable of decreasing IFT to its minimum where the interface is saturated with surfactants. This result is in good accordance with the speculation that the whole interface can be saturated by 14.2 MA molecules (head area of 0.59 nm^2)(29).

The interaction between MA and Triton was also simulated. Figure 3.13 (a) and

(b) show the initial and final configurations of surfactant molecules at the water/PCE interface. The simulations indicate the two MA molecules included in the simulation are separated by Triton molecules in the final configuration. This result suggests that mixing of the MA and Triton molecules at the interface may be favorable to the minimization of system energy. From all the results discussed above, MD simulation has been shown to have great potential as a tool for investigating phase behavior and visualizing microscale structure at the water/PCE interface.

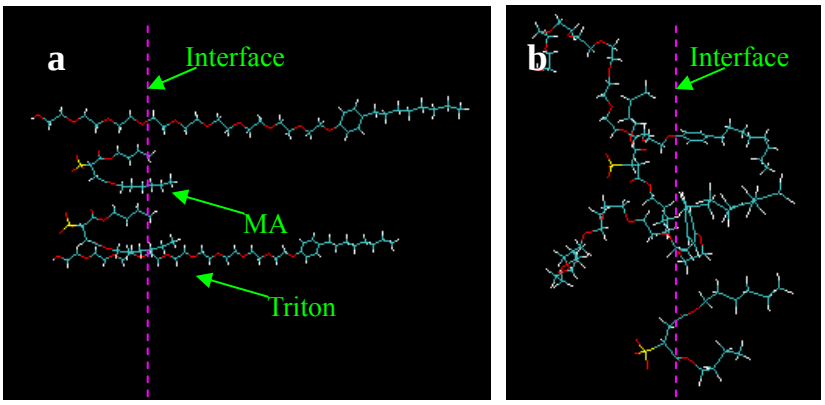

Figure 3.13 MA and Triton molecules at interfaces. Color scheme: yellow, head part of MA; red chain, head part of Triton;

4 SUMARY AND CONCLUSION

The first objective of this work was to investigate the feasibility of using simplified thermodynamic models to describe precipitation conditions for surfactant mixtures in the presence of salt-derived divalent cations. The simulation results show that the model was reasonably accurate for predicting the precipitation boundary of MA/Triton mixtures, despite using fewer parameters than some traditional models. From the simplified model, we can easily predict precipitation by knowing the concentrations of the species involved. For BBRTs, this model can assist in predicting the upper limit of the brine concentration before precipitation occurs. Surfactants also sorb to soils and partition into DNAPL, so it is necessary to quantify their effect in order to develop a more precise model. The heterogeneity of real systems would decrease the predictability of surfactant precipitation. Realistic experiments may be needed to provide empirical knowledge for guiding modifications to model so that the new model would be more applicable to field conditions.

The second objective of this work was to use MD models to visualize microscale structure, calculate interfacial tension, and compare surfactant performance. A few of the large number of microscale configurations that were visualized were presented. The images demonstrate it is feasible to visualize molecular details by conducting MD simulations. It is not clear how to fully utilize the results of the MD simulations and verify the results against experimental measurements. We only focused on interfacial tension, but ignored issues like partitioning of surfactant into DNAPL, the effect of alcohols commonly used with surfactants, and the effect of divalent cations. Despite these shortcomings, the IFT

determined from a MD simulation of a system containing only water and PCE was in general agreement with IFT measurements (46). The simulations that included surfactant indicated that IFT decreased with surfactant concentration, which is consistent with experimental evidence (44). The next step should be to simulate the relationship between the surfactant concentration in the bulk aqueous phase and the accumulation at the water/DNAPL interface. This is of interest because the bulk aqueous concentration is what can be controlled while IFT controls the desired result (e.g., DNAPL mobilization through IFT reduction).

The third objective of this work is to assess the open issues related to surfactant phase behavior in remediation system. In recent studies, MD methods have provided molecularly detailed information for understanding the underlying physics in some specific surfactant system (25-30). Based upon recent developments and the findings from this work, MD simulation may be useful tool for SEAR and BBRT investigations in the two ways discussed below.

(i) Surfactant selection

For a given application, the surfactant solution should be carefully selected to avoid the failure of SEAR strategies (31). The MD simulations described in this work successfully differentiated between Triton and MA. With advances in computational resources, it will become possible to simulate larger systems and calculate more useful parameters in a shorter time. The search for an optimal surfactant from the hundreds available may become less burdensome in the future. MD simulations can also be used to design surfactants specifically used for SEAR. MD simulations have been used to guide the modification of molecular structure in surfactant design by examining changes in performance (27).

(ii) Surfactant precipitation

Despite the successful prediction of precipitation boundaries in this work, there are still questions that thermodynamic methods fail to address. We assumed that counterion binding fractions on micelles were constant partially because of the difficulties to quantify its variation via thermodynamic methods. MD methods may be a solution to this problem because they can effectively visualize the microscale object of interest (25-30). A possible approach is to perform MD simulations to see what would occur around a surfactant micelle. By comparing the modeling results under different conditions, we could determine how binding varies. We could also obtain evidence of surfactant precipitation and thus derive the precipitation boundary, according to the direct observation of surfactant/counterion aggregates in simulated systems. MD simulations have not been used for investigating surfactant precipitation. Simulations would advance the understanding of the important issues involved in anionic surfactant precipitation in calcium salt solutions.

Despite being challenging, resolving the open issues in the above two fields via MD simulations would provide insight into BBRT and SEAR systems.

REFERENCES

1. Mackay, D. M.; Cherry, J. A. *Environ. Sci. Technol.* 1989, 23, 630.

2. Bedient, P.B.; Rifai, H.S.; Newell, C.J. Ground Water Contamination, Transport and Remediation; PTR Prentice Hall: Englewood Cliffs, NJ, 1994

3. Schaerlaekens, J.; Carmeliet, J.; Feyen, J. *Environ. Sci. Technol*. 2005, 39 (7), 2327-2333.

4. Fountain, J.C.; Klimek, A.; Beikirch, M.G.; Middleton, T. M. J. Hazard. Mater. 1991, 28, 295-311.

5. Ouyang, Y.; Mansel, R.S.; Rhue, R.D. *Ground Water* 1995, 33, 399-406.

6. Knox, R.C.; Sabatini, D.A.; Harwell, J.H.; Brown, R.E.; West, C.C.; Blala, F.; Griffin, C. *Ground Water* 1997, 35, 948–953.

7. Martel, R.; Lefebvre, R.; Gelinas, P. J.; *Journal of Contaminant Hydrology* 1998, 30(1-2), 1-31.

8. Londergan, J.T.; Meinardus, H.W.; Mariner, P.E. *Groundwater Monitoring and Remediation* 2001, 21(4), 57-67.

9. Schaerlaekens, J.; Feyen, J. *Journal of Contaminant Hydrology* 2004, 71(1-4), 283-306.

10. Li, Z.H.; Hong, H.L.; *Water Research* 2008, 42(3), 605-614.

11. Pennell, K.D.; Abriola, L.M.; Weber, W.J. *Environ. Sci. Technol*. 1993, 27, 2332-2340.

12. Miller, C.T.; Hill, E.H.; Moutier, M. *Environ. Sci. Technol.* 2000, 34, 719-724.

13. Hill, E. H.; Moutier, M.; Alfaro, J.; Miller, C. T. *Environ. Sci. Technol.* 2001, 35 (14), 3031-3039.

14. Johnson, D.N.; Pedit, J. A.; Miller, C. T. *Environ. Sci. Technol.* 2004, 38, 5149-5156.

15. Holland, P.M.; Rubingh, D.N. Mixed surfactant systems, American Chemical Society, 1992.

16. Stellner, K.L.; Scamehorn, J.F. *J. Am.Oil Chem. Soc.* 1986, 63, 566-574.

17. Stellner, K.L.; Scamehorn, J.F. *Langmuir*. 1989, 5, 70-77.

18. Stellner, K.L.; Scamehorn, J.F. *Langmuir*. 1989, 5, 77-84.

19. Stellner, K.L.; Amante, J.C.; Scamehorn, J.F.; Harwell, J.H. *J. Colloid Interface Sci.* 1988,123,186-200.

20. Rodriguez, C.H.; Lowery, L.H.; Scamehorn, J.F.; Harwell, J.H. *J. Surf. Deterg.* 2001, 4, 1-14.

21. Fuangswasdi, A.; Charoensaeng, A.; Sabatini, D. A.; Scamehorn, J. F.; Acosta, E. J.; Osathaphan, K.; Khaodhiar, S. *J. Surf. Deterg.* 2006, 9(1), 21-28.

22. Amante, J.C.; Scamehorn, J.F.; Harwell, J.H. *J. Colloid Interface Sci*. 1991,144, 243-253.

23. Moroi, Y.; Motomura, K.; Matuura, R. *J. Colloid Interface Sci.* 1974, 46, 111.

24. Moroi, Y.; Nishikido, N.; Matuura, R. *J. Colloid Interface Sci.* 1975, 50, 344.

25. Luo, M.X.; Mazyar, O.A.; Zhu, Q.; Vaughn; M.W.; Hase, W.L.; Dai, L.L. *Langmuir* 2006, 22, 6385-6390.

26. Luo, M.X.; Dai, L. L. *J. Phys.:Condens. Matter.* 2007, 19, 375109.

27. Lu, L.Y.; Berkowitz, M.L. *J. Phys. Chem. B* 2005, 109 (46), 21725-21731.

28. Schweighofer, K.J.; Essmann, U.; Berkowitz, M. *J. Phys. Chem. B* 1997,101, 3793-3799.

29. Dominguez, H. *J. Phys. Chem. B* 2002, 106, 5915-5924.

30. Senapati, S.; Berkowitz, M.L. *Phys. Rev. Lett.*. 2001, 87(17), 176101.

31. Abriola, L.M.; Drummond, C.D.; Hahn, E.J.; Hayes, K.F.; Kibbey, T.C.G.; Lemke, L.D.; Pennell, K.D., Petrovskis, E.A.; Ramsburg, C.A.; Rathfelder, K.M. *Environ. Sci. Technol.* 2005, 39, 1778-1790.

32. Childs, J.; Acosta, E.; Annable, M.D.; Brooks, M.C.; Enfield, C.G.; Harwell, J.H.; Hasegawa, M.; Knox, R.C.; Suresh, P.; Rao, C.; Sabatini, D.A.; Shiau, B.; Szekeres, E.; Wood, A.L. *Journal of Contaminant Hydrology* 2006, 82, 1-22.

33. Sabatini D.A., Knox, R.C.; Harwell, J.H.; Wu, B. *Journal of Contaminant Hydrology* 2000, 45(1-2), 99-121.

34. Langmuir, D. Aqueous environmental geochemistry, Upper Saddle River, N.J. : Prentice Hall, 1997.

35. Rubingh, D.N. Solution Chemistry of surfactants; Mittal, K.L. ed.; Plenum Press, New York, NY, 1979.

36. Rathman, J.F.; Scamehorn, J. F. *J. Phys. Chem.* 1984, 88, 5807-5816.

37. Shinoda, K. Colloidal Surfactants; Shinoda, K.; Tamamushi, B.; Nakagawa, T.; Isemura, T. Eds.; Academic: New York, 1963.

38. Morrisonb, C.; Laurier L.; Schramma, L.L.; Stasiuk, E. N. *Journal of Petroleum Science and Engineering* 1996, 15(1), 91-100.

39. Senapati, S.; Berkowitz, M.L. *J. Phys. Chem.* B 2003, 107 (47), 12906 -12916.

40. Wang, J.M.; Wolf, R.M.; Caldwell, J.W.; Kollman, P.A.; Case, D.A. *J. Comput. Chem.* 2004, 25, 1157-1174.

41. Gundertofte, K.; Liljefors,T.; Norrby, P. O.; Pettersson, I. *J. Comput. Chem.* 1996, 17, 429.

42. Pathria, R. K. Statistical mechanics, Oxford, New York, Pergamon Press, 1972.

43. Parrinello, M. Rahman, A. *J. Appl. Phys.*1981, 52(12),7182-7190.

44. Berendsen, H. J. C.; Postma, J.P.M.; Van Gunsteren, W.F.; Dinola, A.; Haak, J.R. *Journal of Chemical Physics* 1984,81 (8),3684-3690.

45. Demond, A.H.; Lindner, A.S**.** *Environ. Sci. Technol*. 1993, 27 (12), 2318-2331.

46. Jeong, S.W.; Wood, A. L.; Lee, T. R. *J. Hazard. Mater.* B 2002, 95,125–135

47. Walker, R. C.; Hofstee, C.; Dane, J. H.; Hill, W. E. *Journal of Contaminant Hydrology* 1998, 34(1-2), 17-30.